# Azithromycin-Chitosan Films for Improved Haemostasis and Wound Healing

Linda Fateh[1,2*], Susan Waiss[2] and Mohammad Othman[1]

[1]*Department of Pharmaceutics and Pharmaceutical Technology, Faculty of Pharmacy, Damascus University, Syria*

[2]*Scientific Studies and Research Centre, Damascus, Syria*

**Abstract:** Wound healing is a global medical concern, because haemorrhage is still a major cause of morbidity and mortality. Therefore, more effective and cost-effective dressings are required. Antimicrobial dressing of Azithromycin (AZM) (a broad-spectrum macrolide antibiotic) with Chitosan (CS) as a carrier, has a lot of desired properties such as haemostatic, pain-reducing, and less scar forming. It is prepared by a solvent evaporation method. The film morphology is investigated by SEM and film-water wettability is measured by a contact angle method. The drug-polymer interactions are evaluated by using FTIR and DSC. Azithromycin loaded films (different mass ratio of AZM to CS w % 10%, 25% and 50%) were sterilized by Gamma radiation, then their antimicrobial characteristics and haemostatic performance were evaluated. Film thickness was about 9 µm. The wettability properties of films were enhanced by adding AZM and PEG6000 5% (mass ratio of PEG 6000 to CS w %). Microbial growth inhibitions were identified for films loaded with Azithromycin.

**Keywords:** Azithromycin AZM, Chitosan CS, wound healing, haemostatic, film.

## 1. INTRODUCTION

In spite of the development and marketing of several haemostats during the last few decades [1], death from haemorrhage remains a main worldwide problem. Death from haemorrhage represents nearly half of the potential life lost caused by cancer [2], and it is still the main reason of preventable death in combat and civilian trauma situations, despite the varying mechanisms of injuries [3]. Moreover, haemorrhage is a potential complication of any surgical procedure [1]. In everyday life, first-aid knowledge recommends people to apply direct pressure on the wound or cut with a clean cloth, tissue, or piece of gauze, until bleeding stops. However, because of the lack of haemostatic functions, these materials cannot arrest haemorrhage threat. To ensure the survival of patients with massive bleeding, it is essential to achieve quick and absolute haemostasis for pre-hospital care [2].

Haemostasis is still an understudied topic in the surgical field. Therefore, current practice is based on beliefs and habits rather than on evidence, in other words, a so-called 'gold standard' for topical haemostasis does not exist [4]. Haemostatic agents are designed to arrest bleeding through an accelerated promotion of clotting in lesser possible time [5]. Haemostatic agents are particularly useful for patients who require large split skin graft harvests, burn wound debridement, or for other reasons where minimization of topical blood loss is preferred [4]. The essential parameters for an ideal haemostat are the safety, efficacy, ease of use, cost-effectiveness, manufacturability, and biocompatibility, which, however, cannot be achieved at the same time for most haemostatic agents or dressings [1, 2].

Wound healing is a global medical concern with several challenges including the increasing incidence of obesity, type II diabetes, and the aging population [6]. Wound healing in skin is a highly coordinated and regulated process. It occurs over the sequential yet overlapping phases of haemostasis, inflammation, proliferation, and remodeling (Figure **1**) [7]. Any interruption or interference to these phases results in a nonhealing or "stalled" wound, rendering the wound chronic [8]. The main goals of wound care and management are the prevention of infection, maintenance of a moist environment, protection of the wound and achievement of rapid and complete healing with the minimum scar formation [9].

Systemic administration of antimicrobials is not thought to be necessary nor useful for the management of local wound infections, since the drugs may not penetrate well into the wounds (due to lack of blood flow and the presence of dead tissue) or would need to be used in very high doses. Finally, systemic administration has not been shown to prevent bacterial colonization. Furthermore, inappropriate use of

*Address correspondence to this author at the Department of Pharmaceutics and Pharmaceutical Technology, Faculty of Pharmacy, Damascus University, Damascus, P.O. Box 31983, Syria; Tel/Fax: +963 11 223 4947; E-mail: linda.fateh90@damascusuniversity.edu.sy
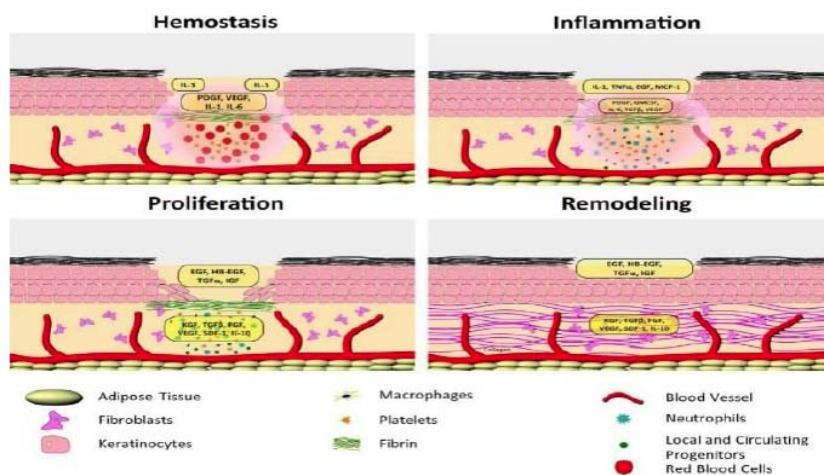
**Figure 1:** Phases of cutaneous wound healing depicting the cells and molecules responsible for the regaining of a healthy barrier [7].

systemic antibiotics can be associated with problems of allergy, toxicity and the development of resistance in non-target organisms [10]. Topical treatment using pharmacological agents, is an effective and safe approach to manage wound pain. Medicated dressings can perform the two essential functions: the treatment of the cause (e.g., wound infection) and the management of the actual wound pain. The treatment of wound infection should result in a reduction in pain, by reducing the bacterial load and thereby reducing the inflammatory stimulus to the nervous system [6]. The majority of primary skin infections are caused by Staphylococcus aureus [11].

Several investigators have confirmed the utility of polymeric film as a drug delivery carrier to avoid hepatic first-pass metabolism and to reduce side effects related to other dosage forms. Furthermore, using films as carrier attains some other goals such as enhancing the bioavailability, realizing controlled/ sustained and/or targeted drug release, minimizing drug dosage, and elevating patient compliance [12].

Chitosan (CS) is considered as one of the most effective antibacterial bio-polymers [13]. CS is a cationic natural polymer. Owing to its haemostatic, stimulation of healing, antimicrobial activity, biocompatible and biodegradable properties, it has been widely used as a topical dressing in wound management [9,14]. The mechanism by which it promotes haemostasis is known to involve the agglutination of blood proteins and platelet activation, for encouraging fibrin clot formation, possibly due to the intrinsic polycationic properties of CS and its nonspecific binding to cell membranes [9]. The polycationic nature of chitosan allows explaining CS analgesic effects, indeed, the amino groups of the D-glucosamine residues could be protonated in the presence of proton ions that are released in the inflammatory area, resulting in an analgesic effect [15]. CS depolymerizes gradually releasing N-acetyl-β-d-glucosamine; this process initiates the proliferation of fibroblasts, helps in ordered collagen deposition, and stimulates an increased level of natural hyaluronic acid synthesis at the wound site, resulting in faster wound healing and scar prevention [14]. CS can accelerate collagen synthesis and efficiently incorporate into fibroblast growth factor, which can improve the wound healing process [16]. Chitosan has recently gained regulatory approval in the USA for use in bandages and other haemostatic agents, because of its properties of binding with red blood cells allowing to form a clot [17]. Therefore, CS is a good candidate for wound dressing. CS-based materials have been prepared as fibers, hydrogels, membranes, sponges, and scaffolds for wound dressing applications [14].

Azithromycin (AZM) which is a semisynthetic acid-stable erythromycin derivative [18], with a long half-life and excellent tissue penetration [19], is classified as the first member of the azalide class and has antibacterial activity and pharmacokinetic profile better than that of erythromycin [20]. This drug acts as a bacteriostatic or bactericidal agent by binding to the 50s ribosomal subunit of susceptible microorganism, and interfering with microbial protein synthesis, and it is effective against gram-negative or gram-positive micro-organisms [21,22]. Moreover, it displays immunomodulatory and anti-inflammatory properties [23]. Azithromycin AZM is a class IV/II BCS drug (WHO, 2005) [24]. A major disadvantage of AZM is its poor solublility in aqueous environmets ($\cong$0.1 mg/mL) [25], AZM has an absolute oral bioavailability of 35−42% [19]. AZM is a potent antibiotic with no

registered topical formulation. (Rukavina *et al.*, 2018) developed Azithromycin loaded liposomes for topical treatment of MRSA (Methicillin-Resistant *Staphylococcus aureus*) infections in wounds [11]. However, according to the best of our knowledge, there is no research which discussed the combination between AZM and CS, subsequently the potential synergistic effects.

Skin injury includes a local loss of stratum corneum leading to altered pH values in wounds compared to skin with an unimpaired barrier function. Because of the lacking stratum corneum function, higher pH values were detected about pH: 7.44 [26]. (Roberts *et al.*, 2005) demonstrated that wounds with a high pH had a lower healing rate by comparison with wounds with a pH closer to neutral [8]. Whereas, the average skin surface pH goes from 4.0 up to 6.3 as reviewed by (Lambers *et al.*, 2006) [26]. An acidic environment is considered favorable for inducing fibroblast proliferation, promoting epithelization and angiogenesis, controlling bacterial colonization and facilitating the release of oxygen from oxyhaemoglobin [27].

Dressings that directly or indirectly reduce the pH of wound fluid may help to prevent infection for rapid healing [8]. Therefore, using chitosan may be beneficial in the prevention and treatment of bacterial colonization [10]. Incorporating of AZM into a polymeric film of chitosan was considered to enhance their antibacterial effects and improve wound healing.

## 2. MATERIALS AND METHODS

### 2.1. Materials

Azithromycin dihydrate, Zhejiang Guobang Pharmaceutical Co., Ltd, (China). The drug is commonly available in the form of dihydrate (MW 785, log P=3.98) [11]. Antimicrobial Disks Azithromycin (15 µg) Abtek biologicals Ltd, Liverpool, UK. Chitosan medium molecular weight (M) Sigma Aldrich, Glacial acetic acid, Polyethylene glycol 6000, ethanol, Calcium chloride, sodium hydroxide, Monobasic Potassium Phosphate. Surgicel® Absorbale haemostat (oxidized regenerated cellulose) (Johnson & Johnson Medical Medical Limited) Switzerland.

### 2.2. Methods

#### 2.2.1. Preparation of Films

Films were prepared by a solvent evaporation method. Chitosan solution 1% (w/v) was prepared by dissolving chitosan powder in 1% (v/v) glacial acetic

acid. The solution was continuously stirred with a magnetic bar for 24 hours, and undissolved impurities and foams removed via centrifuging [28]. PEG 6000 (5% mass ratio to CS w %) and AZM powder at different mass ratio of AZM to CS w% (10%, 25% and 50%) were added to 10 ml of the previously prepared solution and stirred for further 30 min. Chitosan 1% (w/v) solutions and AZM–chitosan dispersions (5 ml) were poured into glass petri dishes (Pyrex® Brand, internal diameter 9 cm), covered with an inverted funnel, and allowed to dry overnight. After drying, the samples were collected and stored in desiccators until further use [29].

#### 2.2.2. Morphological Analysis and Water Contact Angles

The morphology of the film prepared with chitosan (1% w/v) and AZM (the highest prepared concentration was 50%) was observed by scanning electron microscopy (SEM), using (Tescan Vega-II XMU SEM) which operated at 15 kV accelerating voltage. For the top-view image, the sample was attached to the carbon strips without any further procedures. For cross-section image, it was fixed in a vertical position.

To determine the surface wettability, Water Contact angles of the prepared films (CS alone and CS: 50%AZM with 5% PEG 6000) were measured by Digi Scope Digital Microscope, supplied with a digital camera (promate type). Briefly, a droplet of distilled water (3µl) was placed onto the film surface (triplicate samples) and the corresponding contact angles were measured using imageJ software. The maximum volume, whose profile as a sphere shape, was about 3-5 µl. For bigger drops, the other possible approaches are to use some correction factors, or to apply another model called ADSA which calculates the angle by applying the Laplace equation on the profile when profiles are strongly modified by the gravity [30].

#### 2.2.3. Differential Scanning Calorimetry (DSC) Analysis

DSC analysis was performed using a differential scanning calorimeter, DSC131 (SETARAM, France). DSC method consisted of a heating rate of 10 °C.min$^{-1}$ in the range of 25 –350°C. Precisely weighted samples of 5mg were placed in aluminum pans, sealed and perforated with a pin. An empty sealed perforated aluminum pan was used as a reference.

#### 2.2.4. Fourier-Transform Infrared Spectroscopy (FT-IR)

Compact disks of the pure AZM, Chitosan, PEG6000, and physical mixtures were prepared for FT-

IR analysis via KBr disk method. The films were fixed on the support directly in the path of the optical beam. The spectra were obtained by using BRUKER-VECTOR-22 (Billerica, MA, USA). The scanning range was 4000-400 $cm^{-1}$, and the resolution was 2 $cm^{-1}$.

### 2.2.5. In-Vitro Antibacterial Activity

The antibacterial activity of the films against *S. aureus* was determined by a disc diffusion method. Briefly, the bacterial strain isolated from patients was preserved in BRAIN HEART INFUSION BROTH: Glycerol 1:1 at -20 °C. After purification, it was activated on Tryptic soy agar then incubated for 24h at 35±2°C.

After incubation, 4 to 5 isolated bacterial colonies of the stock culture were suspended in sterile saline until the turbidity was compatible with 0.5 MacFarland. A 90 µL of S. aureus suspension was spread onto a Mueller–Hinton agar plate. The films (6 mm) with various concentrations of azithromycin (10, 25, and 50 mg, in triplicates) with fixed content of CS1% w/v and 5% w/w PEG 6000 were pasted onto the agar plate and incubated for 18 h at 35±2 °C. All the samples were exposed to UV 254 nm for 30 min before they were pasted. Membranes without azithromycin were used as a negative control and azithromycin antimicrobial susceptibility disks (15 µg) were used as the positive control. The bacterial growth on the plate was visualized directly, after incubation of the plates at 35±2 °C for 18 h, and the diameter of the inhibition zone was measured according to clinical and laboratory standards institute (CLSI M02-A10) recommendations [23].

### 2.2.6. Haemostatic Performance

#### Coagulation Time

Following a previously established protocol, coagulation times of CS, CS: PEG, CS: PEG: AZM with 10% mass ratio of AZM to CS w% films were tested. 1.0 × 1.0 $cm^2$ of each film in 2 ml Eppendorf plastic tube was placed in a 37°C water bath. Blood alone was the negative control. Whereas, Surgicel® was the positive control. Blood was drawn from voluntary human ulnar vein and mixed with anticoagulant sodium citrate 3.8% at a ratio of 9:1. 100µL of room temperature citrated whole blood was recalcified using a 0.2 M $CaCl_2$ stock to achieve a final $CaCl_2$ concentration of 10 mM, vortexed, and added to each sample. Time was recorded right after addition of 10 µL of 0.2 M $CaCl_2$ aq. solution to the blood. The tube was tilted every 10 sec to observe if the blood was gelatinized. Coagulation was defined as when the entire sample was stagnant during inversion. Each sample was repeated 6 times [31-33].

#### Whole Blood Clotting

The blood clotting studies were directed based on reported literature [32-35]. The blood clotting efficiency (haemoglobin binding) of the CS, CS:PEG, CS: PEG: AZM with 10% mass ratio of AZM to CS w% films, Surgicel® (Johnson & Johnson Medical, USA), and commercial gauze were tested for this study, and each sample was placed in an individual 15-mL plastic Petri dish. Triplicate samples of each film with uniform size of 1.0 × 1.0 $cm^2$ were studied, as follow:

1. Blood was drawn from voluntary human ulnar vein and mixed with anticoagulant sodium citrate 3.8% at a ratio of 9:1.

2. A 100 µl of this blood was slowly dropped to each sample, which was followed by the addition of 10 µL of 0.2 M $CaCl_2$ solution to initiate blood clotting.

3. These specimens were then incubated at 37° C for 15 min. Subsequently, 10 mL of water was added drop by drop gently to haemolyze the red blood cells (RBCs), that were not trapped in the clot, and the absorbance of the resulting haemoglobin solution was measured by an ultraviolet spectrophotometer (OPTIMA SP3000 Plus, Tokyo, Japan) at 540 nm, which corresponded to the amount of haemolyzed red blood cells, that were not incorporated into the clot. The content of haemoglobin in solution was measured by the following equation (1):

   Haemoglobin absorbance% =(Is/Ir)×100, where Is represents the absorbance of the sample and Ir represents the absorbance of the reference value [36].

4. The absorbance of 100 µl of whole blood with 10 µL of 0.2 M $CaCl_2$ in 10 mL of distilled water was applied as a reference value (Blank). A higher absorbance value of the haemoglobin solution thus indicates a slower clotting rate [37].

### 2.2.7. Statistical Analysis

Data was presented as mean ± standard deviation. Statistically significant differences ($p < 0.05$) and extraordinary significant difference ($p < 0.01$) between experimental groups were determined by a Student's t-test and one-way ANOVA, followed by a Tukey test with IBM SPSS 25.

## 3. RESULTS AND DISCUSSION

### 3.1. Preparation of Films

The prepared films were homogenous, translucent and easily removed from the petri dishes.

### 3.2. Morphological Analysis and Water Contact Angles

The digital photographs of the prepared films containing CS alone or CS: AZM 50%: PEG 5% "plasticizer", are shown in Figure **2-1**. The contact angles of these films were measured, in order to characterize the hydrophilicity or hydrophobicity of chitosan-based films. The contact angles of these two films were 85°±1.7 for CS and 35°±2 for CS: AZM with 5% PEG6000.

The top view microscopic and SEM images in Figure **2-2** and **2-3b**, respectively, show that the films produced from medium molecular weight chitosan, alone or with AZM and PEG6000, have relatively flat surfaces.

The cross-section of CS: AZM with 5% PEG6000 film reveals that the thickness was about 9μm (Figure **2-3a**).

The same result for contact angle was reported in the literature for CS samples, which displayed a slightly hydrophilic behavior with a contact angle in the 82° and 86° range [38].

### 3.3. Differential Scanning Calorimetry (DSC) Analysis

Figure **3** illustrates the DSC thermograms of:

(A)  (a) chitosan (CS), (b) Azithromycin (AZM), (C) CS+AZM physical mixture and (d) CS: 5% PEG: 50%AZM Film.
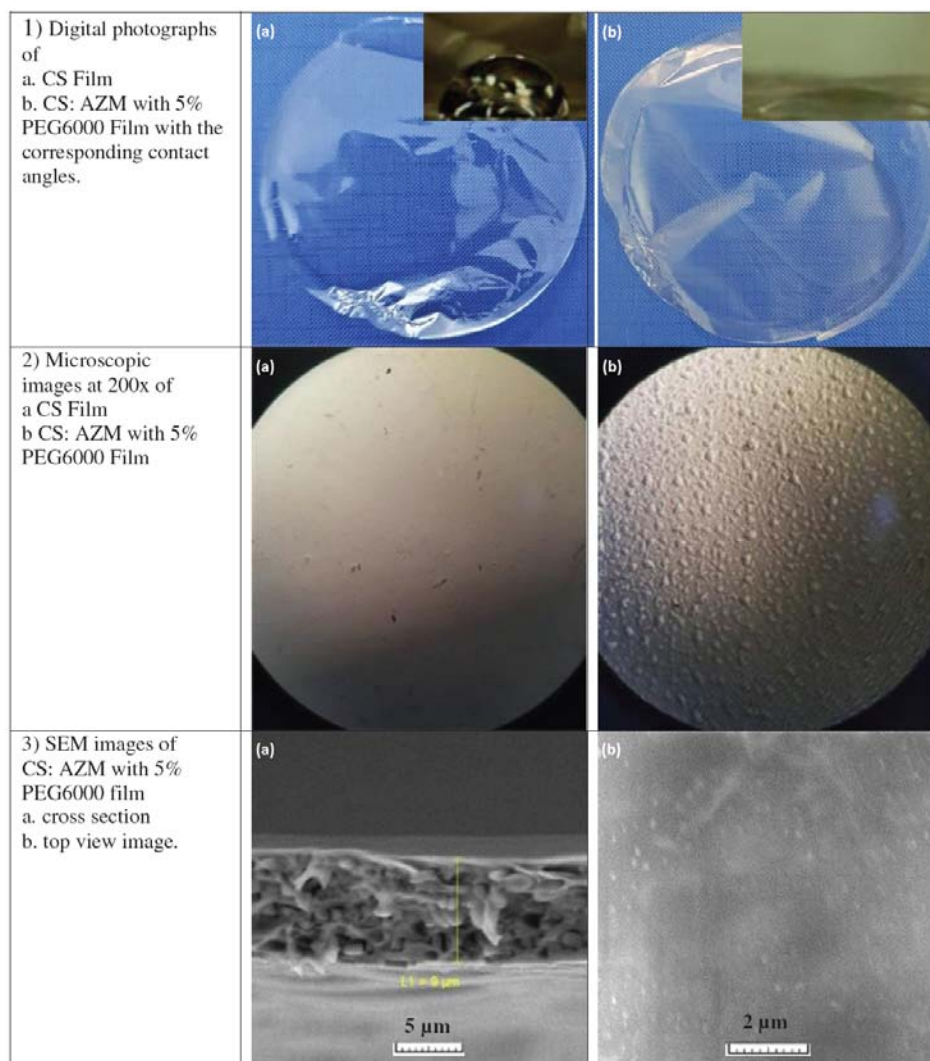


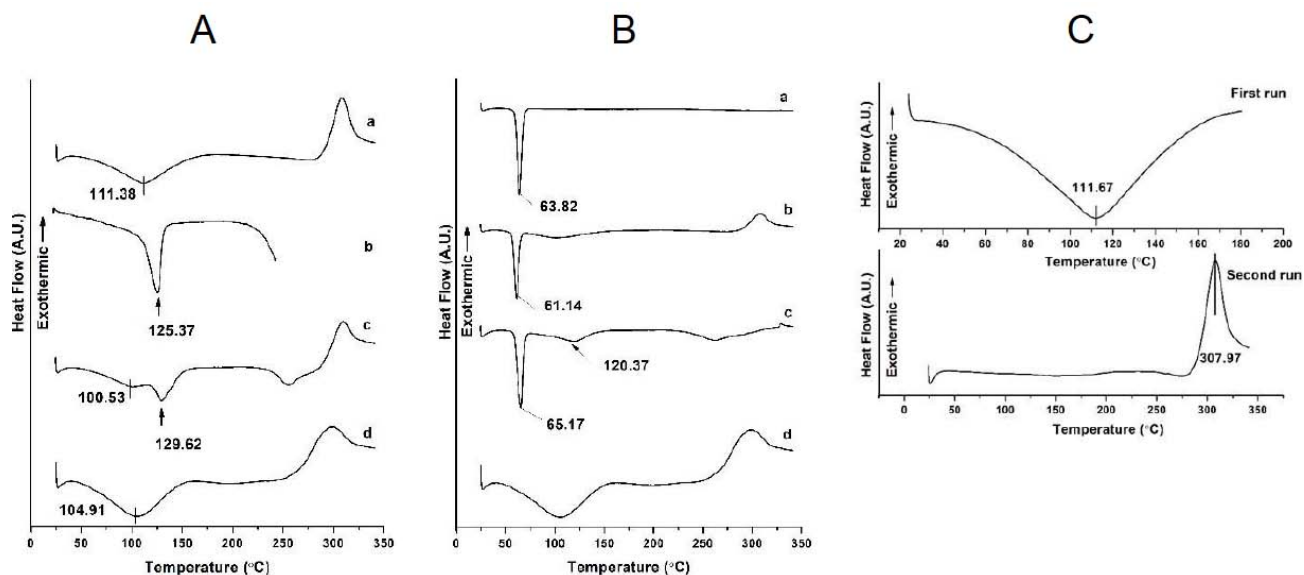**Figure 2:** Morphological analysis of CS and CS: AZM with 5% PEG6000 FILMs.

(B)   (a) PEG6000, (b) PEG+CS physical mixture, (c) PEG+AZM physical mixture and (d) CS: 5% PEG: 50%AZM Film.

(C)   DSC thermograms of CS (as flakes) a) first run (25° – 180° C), b) second run (after cooling to 25° – 300° C).

As shown in the Figure **3A**, the first heating traces at the temperature range from 25° to 350° C, for pure CS, AZM, CS+AZM physical mixture 1:1 and CS based film with AZM 50% samples, all DSC thermograms that contain CS indicated two transitions. The first one, an endothermic event in the temperature range of (100°-120° C) is for dehydration of water molecules [39, 38]. For pure CS, the endothermic event was not detected in the second DSC run (as shown in Figure **3C**) confirming the hypothesis that water evaporation occurred during the first cycle. [38] The second transition at higher temperatures (298°-308° C) is for decomposition of CS. According to (Tripathi *et al.,* 2009), DSC thermogram of chitosan exhibited a sharp exothermic peak at 290° C, associated with the decomposition of chitosan [39]. The thermal behavior of chitosan, and especially its glass transition temperature (Tg), has been the subject of controversy. Apparently, variables such as the source or the extraction method strongly influence Tg (Neto *et al.,* 2005). It was observed that the Tg of chitosan at 203° C (Sakurai *et al.,* 2000), while (Kittur *et al.,* 2002) found no evidence for Tg, suggesting that Tg for chitosan could lie at a higher temperature, where degradation prevents its determination. The same results were

found with (Bonilla *et al.,* 2014), where chitosan did not show any significant transition in the temperature range (25°- 220° C) of the DSC scans at the second heating run [39].

DSC was used to determine different melting points and possible interactions between constituents. AZM and PEG6000 melting peak can be seen in Figure **3A** (b) at 125° C, and in Figure **3B** (a) at 64° C, respectively. DSC thermogram of AZM and PEG 6000 mixture exhibited endothermic melting points at 120° C and 65° C, respectively, as shown in Figure **3B** (c). In the physical mixture, a notable depression of $T_m$ (melting temperature) value of AZM was found, which points out to the good miscibility of AZM with PEG that affect crystallization of AZM. This reduction of the crystallization or melting temperature is considered as a measure of the blend compatibility [40]. For CS and PEG mixture, a notable depression of $T_m$ value of PEG was found, as shown in Figure **3B** (b).

The first transition of (CS+AZM) was observed with two endothermic peaks, the first at 100° C and the second at 129° C. The second transition with an endothermic peak at 255° C, and the third transition with an exothermic peak at 309° C, which indicate no interactions between them as a physical mixture, as shown in Figure **3A** (c). Whereas on film thermograms, the AZM melting peak did not appear. AZM and CS behaved as a single entity, with one melting point (dehydration) around 105° C, as shown in Figures **3A** (d), **3B** (d). The reason for the absence of the endothermic peak of AZM could be that the drug would



**Figure 3:** DSC thermogram of (**A**) (a) chitosan (CS), (b) Azithromycin (AZM), (C) CS+AZM physical mixture and (d) CS: 5% PEG: 50%AZM Film. (**B**) (a) PEG6000, (b) PEG+CS physical mixture, (c) PEG+AZM physical mixture and (d) CS: 5% PEG: 50%AZM Film. (**C**) DSC thermograms of CS (as flakes) a) first run, b) second run.
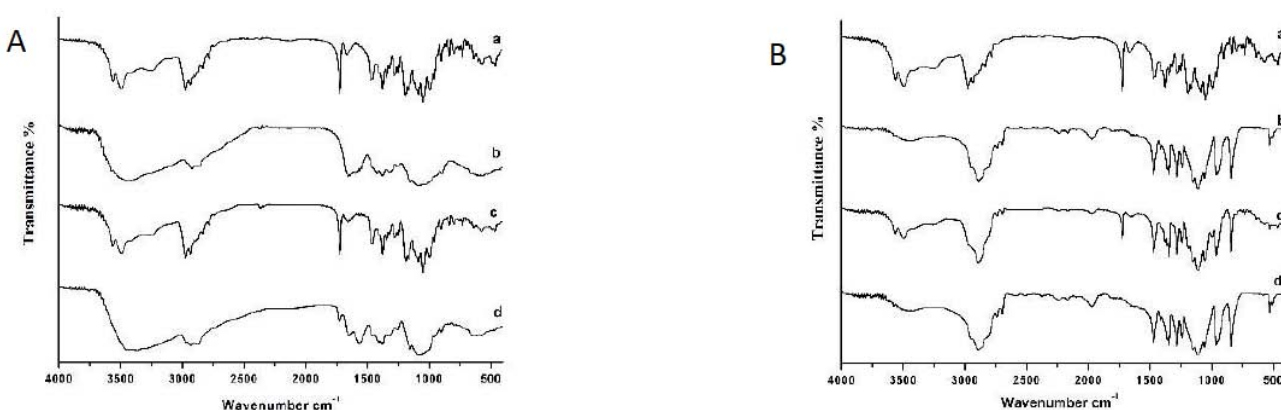
**Figure 4:** FTIR **A** (a) AZM (b) CS (c) AZM: CS physical mixture (d) CS: 5% PEG: 50%AZM Film. **B** (a) AZM (b) PEG6000(c) PEG: AZM physical mixture (d) CS: PEG6000.

dissolve and distribute within the carrier and convert from crystalline to amorphous form [24].

## 3.4. Fourier-Transform Infrared Spectroscopy (FT-IR)

FTIR spectral analysis was carried out for the structural characterization of AZM, CS, CS-AZM physical mixture, and CS: 5% PEG: 50%AZM Film. As well as FTIR spectra of AZM, PEG6000, their physical mixture and CS: PEG6000 physical mixture, as shown in Figure **4**.

The FTIR spectrum of AZM in Figure **4A** (a) displays characteristic sharp peaks at 3567, 3496 and 3236 cm$^{-1}$, which represents free hydroxyl, hydrogen bonded hydroxyl and intramolecular hydrogen bonded hydroxyl functional groups, respectively [25]. A sharp peak at 3463 cm$^{-1}$ corresponds to free O-H stretching indicative of the presence of tightly bound water in the crystal lattice [23]. IR spectrum of the PEG 6000 also displayed characteristic peaks at 3244 cm$^{-1}$ (O-H stretch), 2907 cm-1 (for C-H stretch), and 1108 cm$^{-1}$ (for C-O-C stretch) [41] (Figure **4B**). In physical mixtures, no interactions between drug and polymers were observed. The main peaks of the drug and polymers were clearly distinguished in physical mixtures. In azithromycin loaded CS film, the broad band at 3600–3300 cm$^{-1}$ (less intense peak compared

with AZM) is due to the O-H stretching of the loosely bound water characteristic of the amorphous phase [23].

## 3.5. *In-Vitro* Antibacterial Activity

Bacterial infections of the skin and soft tissues are the most frequent disorders encountered in acute ambulatory care, and the majority of primary skin infections are caused by *Staphylococcus aureus* [11].

As presented in Table **1** A: When the film AZM15µg:CS: PEG5% contains the same amount of drug as in the disk (Antimicrobial disk AZM 15µg), it has a broader inhibition zone (25.8±0.22 mm) than the positive control (23.1±0.9 mm). Furthermore, a negative control, consists of a film without azithromycin, has demonstrated antimicrobial activity with inhibition zone, its diameter about 12 mm, which can be explained by the antimicrobial properties of CS.

Figure **5** shows that the antimicrobial properties of AZM, when loaded into CS film with different mass ratio of AZM to CS (10%, 25%, 50%), was superior to that of Antimicrobial disk AZM 15µg (the positive control). The corresponding inhibition zone diameters in mm presented in Table **1** B: for CS: AZM10%: PEG5%, CS: AZM 25%: PEG5%, CS: AZM50%: PEG5% are 30.9±0.7, 32±0.15, 33.2±0.4 respectively.

**Table 1:   Inhibition Zones Diameter of the Films**

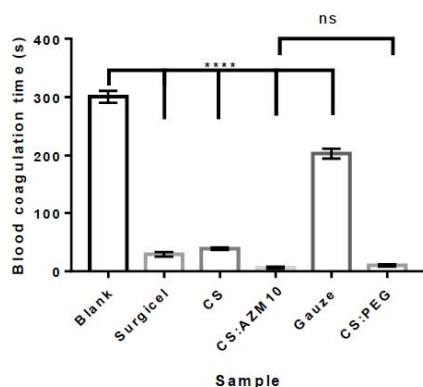| A | AZM 15 µg:CS: PEG5% | CS: PEG 5% (- control) | Antimicrobial disk AZM 15µg (+ control) | |
|---|---|---|---|---|
| Inhibition zones diameter in mm | 25.8±0.22 | 11.8±0.2 | 23.1±0.9 | |
| B | CS: AZM10%: PEG5% | CS: AZM 25%: PEG5% | CS: AZM 50%: PEG5% | Antimicrobial disk AZM 15µg |
| Inhibition zones diameter in (mm) | 30.9±0.7 | 32±0.15 | 33.2±0.4 | 23.1±0.9 |

**Figure 5:** Inhibition zones against S.*aureus* for: (1) CS:AZM10% (2) CS:AZM 25% (3) CS:AZM 50% (4) Antimicrobial disk AZM 15µg.

The drug bioactivity was well preserved despite the amorphous transformation that occurred during the preparation of the film. Similar results were found when (Mathew *et al.,* 2017) developed a calcium phosphate (CaP), coated with medical grade polycaprolactone (mPCL) electrospun membrane and loaded with azithromycin, for local and controlled drug delivery [23]. The antimicrobial mechanism of chitosan was attributed to the interaction with the strongly electronegative microbial surface [42], which explains the inhibition zone for CS film even without AZM, and the superior antimicrobial properties for AZM:CS film. Furthermore, it could be attributed to the diffusion of AZM from the film.

### 3.6. Haemostatic Performance

#### *Coagulation Time*

As rapid haemostasis is essential as a strategy not only for initial survival but also for optimal recovery [31],
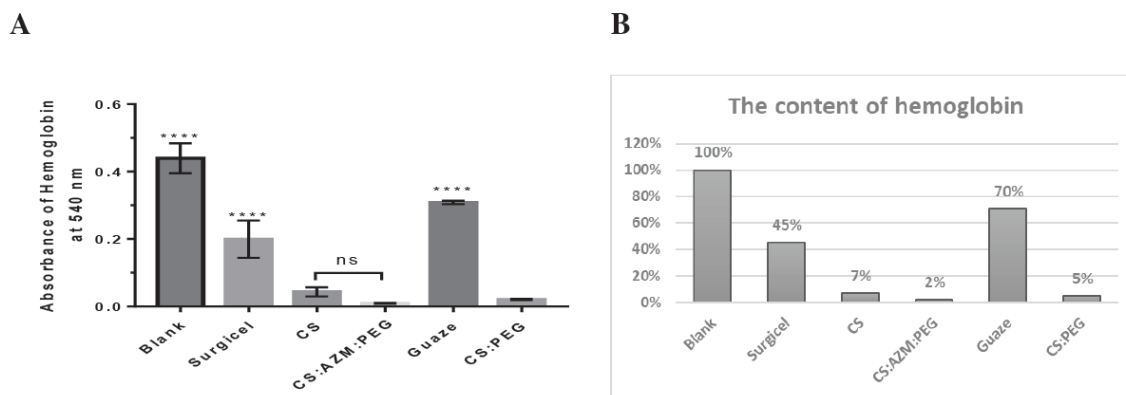
the coagulation time was investigated. For CS, CS: AZM: PEG, CS: PEG films, Blank (negative control), and Surgicel® (positive control), the corresponding coagulation times are shown in Figure **6A**, and photographs of the clots formed in both blank (left) and CS: AZM: PEG (right) blood tubes are shown in Figure **6B**.

The blood coagulation time for CS alone was about 40 sec, while for CS: AZM10%: PEG5% and CS: PEG5%, it was about 10 sec, which was superior to Surgicel® that can be explained by the hydrophilicity enhancement after the addition of PEG, and this indicates no interaction between AZM and CS that influences the haemostatic properties of chitosan.

#### *Whole Blood Clotting*

In order to evaluate the haemostatic potential of the prepared films, a whole-blood clotting study was conducted. Figure **7** shows the corresponding absorbance of haemoglobin from haemolyzed uncoagulated RBCs that resulted from the same samples, as well as the percentage of blood clotting induced by the CS, CS: AZM: PEG, CS: PEG films, Surgicel® and gauze. A higher absorbance value of the haemoglobin solution indicates a slower clotting rate [33].

As presented from the results, both CS:PEG, CS: AZM:PEG show a better haemostatic effect than that of gauze and Surgicel®, which can be resulted in from: (i) chitosan hydrophilic and belong to ionic species which can induce the platelet coagulation through electrostatic adsorption interactions [33] (ii) Incorporating PEG 6000 as solubility enhancer and plasticizer improve the hydrophilicity and give better haemostatic result.



A: In vitro coagulation time of the prepared films.



B. Photographs of coagulation blood tubes

**Figure 6:** Coagulation time of samples. Where ns (no significance), [****](p value <0.0001).

A

B



**Figure 7:** (**A**) The corresponding absorbance of haemoglobin from haemolyzed uncoagulated RBCs, and (**B**) The percentage of blood clotting enhancement induced by the samples. * Blank: Recalcified citrated whole blood, CS: Chitosan, AZM: Azithromycin, Gauze: Positive control.

## 4. CONCLUSION

Films based on chitosan, and azithromycin incorporated with the addition of PEG6000 as a plasticizer and solubility enhancer, were prepared by a simple solvent-evaporation method. The physicochemical characteristics demonstrated no significant interactions between CS, AZM, and PEG, as indicated by DSC thermograms and FTIR spectra.

DSC thermograms as well as FTIR spectra indicate a transformation of AZM from crystalline to amorphous form in films, the formed films should be kept in good storage conditions. The obtained films were ultrathin, which may be ideal for drug diffusion to the wound areas.

The benefits of this combination were confirmed by antimicrobial and haemostatic performance tests.

The best microbiological and haemostatic results were obtained by films consisting of CS: AZM 10%: PEG5%. The mass ratio of AZM to CS (25, 50%) gave no additional benefits to the mass ratio 10% in antimicrobial studies. Therefore, the least mass ratio (10%) was chosen to complete the study.

According to the previous results, the prepared films might be excellent candidates for infected wound treatment, and at the same time for post injuries applications, because of its unique properties, which are haemostasis effect, pain-reducing, antimicrobial characteristics, and less scar formation.

## FUNDING

## REFERENCES

[1]     Di Lena F. Hemostatic polymers: The concept, state of the art and perspectives [Internet]. Journal of Materials Chemistry B. The Royal Society of Chemistry 2014; Vol. 2: [cited 2019 May 12]. p. 3567-77.
https://doi.org/10.1039/C3TB21739F

[2]     Yu L, Shang X, Chen H, Xiao L, Zhu Y, Fan J. A tightly-bonded and flexible mesoporous zeolite-cotton hybrid hemostat. Nat Commun [Internet]. 2019 Dec 29 [cited 2019 May 6]; 10(1): 1932.
https://doi.org/10.1038/s41467-019-09849-9

[3]     Khoshmohabat H, Paydar S, Kazemi HM, Dalfardi B. Overview of agents used for emergency hemostasis. Trauma Monthly. Kowsar Medical Publishing Company 2016; Vol. 21.
https://doi.org/10.5812/traumamon.26023

[4]     Groenewold MD, Gribnau AJ, Ubbink DT. Topical haemostatic agents for skin wounds: A systematic review. BMC Surg [Internet]. 2011 Dec 12 [cited 2019 May 25]; 11(1): 15.
https://doi.org/10.1186/1471-2482-11-15

[5]     Nakielski P, Pierini F. Blood interactions with nano- and microfibers: Recent advances, challenges and applications in nano- and microfibrous hemostatic agents [Internet]. Vol. 84, Acta Biomaterialia 2019 [cited 2019 Mar 31]. p. 63-76.
https://doi.org/10.1016/j.actbio.2018.11.029

[6]     Boateng J, Catanzano O. Advanced Therapeutic Dressings for Effective Wound Healing - A Review. J Pharm Sci [Internet] 2015; 104(11): 3653-80.
https://doi.org/10.1002/jps.24610

[7]     Hamdan S, Pastar I, Drakulich S, Dikici E, Tomic-Canic M, Deo S, *et al*. Nanotechnology-Driven Therapeutic Interventions in Wound Healing: Potential Uses and Applications. ACS Cent Sci 2017; 3(3): 163-75.
https://doi.org/10.1021/acscentsci.6b00371

[8]     Percival SL, McCarty S, Hunt JA, Woods EJ. The effects of pH on wound healing, biofilms, and antimicrobial efficacy [Internet]. Wound repair and regeneration : official publication of the Wound Healing Society [and] the European Tissue Repair Society 2014; Vol. 22: [cited 2019 May 11]. p. 174–86.
https://doi.org/10.1111/wrr.12125

[9]     Dai T, Tanaka M, Huang YY, Hamblin MR. Chitosan preparations for wounds and burns: Antimicrobial and wound-healing effects [Internet]. Vol. 9, Expert Review of Anti-Infective Therapy. NIH Public Access 2011 [cited 2019 May 25]. p. 857-79.
https://doi.org/10.1586/eri.11.59

[10] Halstead FD, Rauf M, Bamford A, Wearn CM, Bishop JRB, Burt R, *et al*. Antimicrobial dressings: Comparison of the ability of a panel of dressings to prevent biofilm formation by key burn wound pathogens. Burns [Internet]. 2015 Dec [cited 2019 Jun 5]; 41(8): 1683-94.
https://doi.org/10.1016/j.burns.2015.06.005

[11] Rukavina Z, Šegvić Klarić M, Filipović-Grčić J, Lovrić J, Vanić Ž. Azithromycin-loaded liposomes for enhanced topical treatment of methicillin-resistant Staphyloccocus aureus (MRSA) infections. Int J Pharm [Internet]. 2018 Dec 9 [cited 2018 Oct 22]; 553(1-2): 109-19.
https://doi.org/10.1016/j.ijpharm.2018.10.024

[12] Ghosal K, Chandra A, Praveen G, Snigdha S, Roy S, Agatemor C, *et al*. Electrospinning over Solvent Casting: Tuning of Mechanical Properties of Membranes. Sci Rep [Internet]. 2018 Dec 22 [cited 2019 May 22]; 8(1): 5058.
https://doi.org/10.1038/s41598-018-23378-3

[13] Hassan MA, Omer AM, Abbas E, Baset WMA, Tamer TM. Preparation, physicochemical characterization and antimicrobial activities of novel two phenolic chitosan Schiff base derivatives. Sci Rep 2018; 8(1): 1-14.
https://doi.org/10.1038/s41598-018-29650-w

[14] Xu F, Weng B, Materon LA, Gilkerson R, Lozano K. Large-scale production of a ternary composite nanofiber membrane for wound dressing applications. J Bioact Compat Polym [Internet]. 2014 Nov [cited 2019 May 27]; 29(6): 646-60.
https://doi.org/10.1177/0883911514556959

[15] Croisier F, Jérôme C. Chitosan-based biomaterials for tissue engineering [Internet]. Vol. 49, European Polymer Journal. Pergamon 2013 [cited 2019 May 12]. p. 780-92.
https://doi.org/10.1016/j.eurpolymj.2012.12.009

[16] Pilehvar-Soltanahmadi Y, Akbarzadeh A, Moazzez-Lalaklo N, Zarghami N. An update on clinical applications of electrospun nanofibers for skin bioengineering [Internet]. Vol. 44, Artificial Cells, Nanomedicine and Biotechnology 2016 [cited 2019 May 11]. p. 1350-64. Available from: http://www.ncbi.nlm.nih.gov/pubmed/25939744

[17] Gu BK, Park SJ, Kim MS, Kang CM, Kim J Il, Kim CH. Fabrication of sonicated chitosan nanofiber mat with enlarged porosity for use as hemostatic materials. Carbohydr Polym [Internet]. 2013 Aug 14 [cited 2019 Mar 10]; 97(1): 65-73.
https://doi.org/10.1016/j.carbpol.2013.04.060

[18] Gandhi R, Pillai O, Thilagavathi R, Gopalakrishnan B, Kaul CL, Panchagnula R. Characterization of Azithromycin hydrates. Eur J Pharm Sci [Internet]. 2002 Aug 1 [cited 2019 Jul 29]; 16(3): 175-84.
https://doi.org/10.1016/S0928-0987(02)00087-8

[19] McMullan BJ, Mostaghim M. Prescribing azithromycin. Aust Prescr [Internet]. 2015 Jun [cited 2019 Aug 29]; 38(3): 87-9.
https://doi.org/10.18773/austprescr.2015.030

[20] Payab S, Jafari-Aghdam N, Barzegar-Jalali M, Mohammadi G, Lotfipour F, Gholikhani T, *et al*. Preparation and physicochemical characterization of the azithromycin-Eudragit RS 100 nanobeads and nanofibers using electrospinning method. J Drug Deliv Sci Technol [Internet]. 2014; 24(6): 585-90.
https://doi.org/10.1016/S1773-2247(14)50123-2

[21] Azhdarzadeh M, Lotfipour F, Zakeri-Milani P, Mohammadi G, Valizadeh H. Anti-bacterial performance of azithromycin nanoparticles as colloidal drug delivery system against different gram-negative and gram-positive bacteria. Adv Pharm Bull 2012; 2(1): 17-24.

[22] Liang D, Lu Z, Yang H, Gao J, Chen R. Novel Asymmetric Wettable AgNPs/Chitosan Wound Dressing: *In vitro* and *in vivo* Evaluation. ACS Appl Mater Interfaces. 2016 Feb 24; 8(6): 3958-68.
https://doi.org/10.1021/acsami.5b11160

[23] Mathew A, Vaquette C, Hashimi S, Rathnayake I, Huygens F, Hutmacher DW, *et al*. Antimicrobial and Immunomodulatory Surface-Functionalized Electrospun Membranes for Bone Regeneration. Adv Healthc Mater 2017; 6(10).
https://doi.org/10.1002/adhm.201601345

[24] Kauss T, Gaubert A, Boyer C, Ba BB, Manse M, Massip S, *et al*. Pharmaceutical development and optimization of azithromycin suppository for paediatric use. Int J Pharm [Internet]. 2013 Jan 30 [cited 2019 Jul 29]; 441(1-2): 218-26.
https://doi.org/10.1016/j.ijpharm.2012.11.040

[25] Aucamp M, Odendaal R, Liebenberg W, Hamman J. Amorphous azithromycin with improved aqueous solubility and intestinal membrane permeability. Drug Dev Ind Pharm [Internet]. 2015 Jul 3 [cited 2019 Mar 3]; 41(7): 1100-8.
https://doi.org/10.3109/03639045.2014.931967

[26] Schreml S, Szeimies RM, Karrer S, Heinlin J, Landthaler M, Babilas P. The impact of the pH value on skin integrity and cutaneous wound healing. J Eur Acad Dermatology Venereol 2010; 24(4): 373-8.
https://doi.org/10.1111/j.1468-3083.2009.03413.x

[27] Power G, Moore Z, O'Connor T. Measurement of pH, exudate composition and temperature in wound healing: A systematic review. J Wound Care [Internet]. 2017 Jul 2 [cited 2018 Sep 16]; 26(7): 381-97.
https://doi.org/10.12968/jowc.2017.26.7.381

[28] Shuai H-H, Yang C-Y, Harn HI-C, York RL, Liao T-C, Chen W-S, *et al*. Using surfaces to modulate the morphology and structure of attached cells – a case of cancer cells on chitosan membranes. Chem Sci [Internet]. 2013 Jul 2 [cited 2019 May 5]; 4(8): 3058.
https://doi.org/10.1039/c3sc50533b

[29] Habiba U, Afifi AM, Salleh A, Ang BC. Chitosan/(polyvinyl alcohol)/zeolite electrospun composite nanofibrous membrane for adsorption of Cr6+, Fe3+ and Ni2+. J Hazard Mater [Internet]. 2017 Jan 15 [cited 2019 Jul 15]; 322: 182-94.
https://doi.org/10.1016/j.jhazmat.2016.06.028

[30] Contact Angle [Internet]. [cited 2019 Aug 26]. Available from: https://imagej.nih.gov/ij/plugins/contact-angle.html

[31] Sun X, Tang Z, Pan M, Wang Z, Yang H, Liu H. Chitosan/kaolin composite porous microspheres with high hemostatic efficacy. Carbohydr Polym [Internet]. 2017 Dec [cited 2018 Aug 5]; 177: 135-43.
https://doi.org/10.1016/j.carbpol.2017.08.131

[32] Fathi P, Sikorski M, Christodoulides K, Langan K, Choi YS, Titcomb M, *et al*. Zeolite-loaded alginate-chitosan hydrogel beads as a topical hemostat. J Biomed Mater Res - Part B Appl Biomater [Internet]. 2018 Jul 1 [cited 2018 Aug 8]; 106(5): 1662-71.
https://doi.org/10.1002/jbm.b.33969

[33] Tan L, Hu J, Huang H, Han J, Hu H. Study of multi-functional electrospun composite nanofibrous mats for smart wound healing. Int J Biol Macromol [Internet]. 2015; 79: 469-76.
https://doi.org/10.1016/j.ijbiomac.2015.05.014

[34] Gu BK, Park SJ, Kim MS, Lee YJ, Kim J-I, Kim C-H. Gelatin blending and sonication of chitosan nanofiber mats produce synergistic effects on hemostatic functions. Int J Biol Macromol [Internet]. 2016 Jan 1 [cited 2019 Apr 27]; 82: 89-96.
https://doi.org/10.1016/j.ijbiomac.2015.10.009

[35] Madhumathi K, Sudheesh Kumar PT, Abhilash S, Sreeja V, Tamura H, Manzoor K, *et al*. Development of novel chitin/nanosilver composite scaffolds for wound dressing applications. J Mater Sci Mater Med [Internet]. 2010 Feb 3 [cited 2019 Aug 31]; 21(2): 807-13.
https://doi.org/10.1007/s10856-009-3877-z

[36] Quan K, Li G, Tao L, Xie Q, Yuan Q, Wang X. Diaminopropionic Acid Reinforced Graphene Sponge and Its Use for Hemostasis. ACS Appl Mater Interfaces [Internet]. 2016 Mar 30 [cited 2019 Sep 2]; 8(12): 7666-73.
https://doi.org/10.1021/acsami.5b12715

[37]   Ong SY, Wu J, Moochhala SM, Tan MH, Lu J. Development of a chitosan-based wound dressing with improved hemostatic and antimicrobial properties. Biomaterials [Internet]. 2008 Nov [cited 2019 Jun 7]; 29(32): 4323-32. https://doi.org/10.1016/j.biomaterials.2008.07.034

[38]   Ruini F, Tonda-Turo C, Chiono V, Ciardelli G. Chitosan membranes for tissue engineering: Comparison of different crosslinkers. Biomed Mater [Internet]. 2015 Nov 3 [cited 2018 May 26]; 10(6): 065002. https://doi.org/10.1088/1748-6041/10/6/065002

[39]   Thein-Han WW, Saikhun J, Pholpramoo C, Misra RDK, Kitiyanant Y. Chitosan-gelatin scaffolds for tissue engineering: Physico-chemical properties and biological response of buffalo embryonic stem cells and transfectant of GFP-buffalo embryonic stem cells. Acta Biomater [Internet]. 2009 Nov [cited 2019 Jul 21]; 5(9): 3453-66. https://doi.org/10.1016/j.actbio.2009.05.012

[40]   Bonilla J, Fortunati E, Atarés L, Chiralt A, Kenny JM. Physical, structural and antimicrobial properties of poly vinyl alcohol–chitosan biodegradable films. Food Hydrocoll [Internet]. 2014 Mar 1 [cited 2019 Jul 15]; 35: 463-70. https://doi.org/10.1016/j.foodhyd.2013.07.002

[41]   Adeli E. Preparation and evaluation of azithromycin binary solid dispersions using various polyethylene glycols for the improvement of the drug solubility and dissolution rate. Brazilian J Pharm Sci [Internet]. 2016 Mar [cited 2018 Dec 4]; 52(1): 1-13. https://doi.org/10.1590/S1984-82502016000100002

[42]   Li L, Deng J, Deng H, Liu Z, Li X. Preparation , characterization and antimicrobial activities of chitosan / Ag / ZnO blend films. Chem Eng J [Internet]. 2010; 160(1): 378-82. https://doi.org/10.1016/j.cej.2010.03.051